J. Am. Chem. Soc. **1984**, *106*, 4606–4615

Crystal and Molecular Structure of *S*-Deoxo[Ile^3]amaninamide: A Synthetic Analogue of *Amanita* Toxins

G. Shoham,*† D. C. Rees,†,§ W. N. Lipscomb,*† G. Zanotti,‡,⊥ and Th. Wieland‡

Contribution from Gibbs Laboratory, Department of Chemistry, Harvard University, Cambridge, Massachusetts 02138, and Max Planck Institute for Medical Research, Heidelberg, Germany.
Received December 22, 1983

Abstract: The crystal structure of *S*-deoxo[Ile^3]amaninamide, a nontoxic synthetic derivative of the *Amanita phalloides* mushroom toxins (amatoxins), has been determined by single-crystal X-ray diffraction. The crystals are monoclinic, space group $P2_1$, with 2 formula units per unit cell. Cell dimensions are a = 12.147 Å, b = 11.250 Å, c = 19.267 Å, and β = 92.41°. The structure was determined by molecular replacement methods and refined by least-squares techniques to a final R value of 0.065 for 3894 independent observations. Six intramolecular hydrogen bonds hold the bicyclic octapeptide in a compact conformation, which is very similar to the conformation of the naturally occurring (and toxic) amatoxin, β-amanitin. The study demonstrates that the 30-fold reduction in binding affinity to RNA polymerase B of the title amatoxin, and probably of most of the other amatoxin analogues with altered side chain 3, is not due to alteration of backbone conformation. The three water molecules and two ethanol molecules, crystallized with the amatoxin, form a strong and extensive intermolecular hydrogen-bonding system.

Among the poisonous mushrooms, almost all of the deadliest ones are members of the *Amanita* genus. In Europe, 90–95% of all deaths from mushroom poisoning have traditionally been attributed to the green-capped mushroom of that genus—*Amanita phalloides*.[1,2] *A. phalloides* is found mainly in Central Europe[2] but it was discovered recently in several places in North America as well.[3-5] The mushroom contains two families of toxic compounds, the amatoxins and phallotoxins.[6] Both are bicyclic peptides with an unusual sulfur bridge between a tryptophan and a cysteine side chain, and both contain uncommon hydroxylated amino acids. However, their mechanisms of action are different. Amatoxins form a very strong 1:1 complex with RNA polymerase B, which blocks mRNA synthesis in the nucleoplasm, hence stopping protein synthesis in the affected cells.[6,7] Phallotoxins are believed to act by preventing depolymerization of microfilamentous F-actin in liver cells.[6,8]

It is most probable that the phallotoxins play no role in the lethal mushroom poisoning of humans (they are not resorbed by the gastrointestinal tract); it is therefore very likely that amatoxins are the sole cause of death in these cases.[6] A typical sample of *A. phalloides* mushroom contains 3–5 mg of amatoxins[5,9] and 4–6 mg of phallotoxins[6] per gram of dry tissue (corresponding to about 20 g of fresh tissue). Since the lethal dose of amatoxins is lower than 0.1 mg/kg of body weight for humans, it is possible that the toxin content of one mushroom weighing 40–50 g (about 8–12 mg of amatoxins) may be sufficient to kill an adult.[2,6]

Nine different amatoxins have been isolated and characterized from *Amanita* mushrooms[6,10] (six of which are compounds **1–6** in Table I). The general chemical structure of the amatoxin family is depicted in Figure 1, where the specific composition of α-amanitin, the most common member, is indicated. It is a bicyclic octapeptide with a sulfoxide transannular bridge between cysteine-8 and hydroxytryptophan-4 (HyTrp-4).

The X-ray crystallographic study of β-amanitin, performed in this laboratory,[11a,b] elucidated the detailed three-dimensional structure of this compound and its overall conformation in the crystal. The X-ray structure confirmed the proposed chemical structure and absolute configuration of amatoxins. It has been shown that all amino acid residues have the expected L configuration and all peptide bonds are trans. The bicyclic frame was shown to be rather rigid and to be held by four intramolecular hydrogen bonds (two strong and two weak). A NMR study on the conformation of α-amanitin in Me_2SO solution[12] demonstrated that the structure of α-amanitin in solution is similar to the structure of β-amanitin in the crystalline state.

In addition to the naturally occurring amatoxins, about 40 chemically modified and synthetic amatoxin derivatives have been reported,[6,13] all retaining the basic bicyclic frame with minor changes in side chains (including compounds **7–10** in Table I). Most of these natural amatoxins and the synthetic analogues exhibit a rather high binding affinity to RNA polymerase B (K_i < 10^{-8} M) and in vivo toxicity ($LD_{50} \approx 0.5$ mg/kg of white mouse) as illustrated in Table I. In contrast, some derivatives, usually differing from the active ones only by one or a few functional groups, lose their toxicity while maintaining most of their binding capacity (e.g. and **4** and **7**), or display substantial reduction in both the binding capacity and toxicity (e.g., **5** and **10**).

A typical example is the role of the two hydroxy groups of the γ,δ-dihydroxyisoleucine side chain (Dihylle-3). It was shown[6] that the lack of the δ-hydroxy group has no effect on either the binding constant to the enzyme or the in vivo toxicity (e.g., **3**), whereas removal of the γ-hydroxy group reduces the binding capacity by factors of 4–15[6,13] and diminishes the toxicity almost completely (e.g., **4** and **10**).

† Harvard University.
‡ Max Planck Institute for Medical Research.
§ Present address: Department of Chemistry, University of California, Los Angeles, CA 90024.
⊥ Present address: Centro di Chimica del Farmaco del Consiglio Nazionale delle Ricerche, Università di Roma, Italy.

(1) Wieland, Th., Science, (*Washington, D. C.*) **1968**, *159*, 946.
(2) Wieland, Th.; Wieland, O. In "Microbial Toxins"; Kadis, S., Cigler, A., Ajl, S., Eds.; Academic Press: New York, 1972, Vol. 8, pp 249–280.
(3) Simons, D. M. *Del. Med. J.* **1971**, *43*, 177.
(4) Tanghe, L. J.; Simons, D. M. *Mycologia* **1973**, *65*, 99.
(5) Yocum, R. R.; Simons, D. M. *Lloydia* **1977**, *40*, 178.
(6) Wieland, Th.; Faulstich, H. *CRC Crit. Rev. Biochem.* **1976**, *5*, 185.
(7) Cochet-Meilhac, M.; Chambon, P. *Biochim. Biophys. Acta* **1974**, 353, 160.
(8) Lengsfeld, A.; Löw, I.; Wieland, Th.; Dancker, P.; Hasselbach, W. *Proc. Natl. Acad. Sci. U.S.A.* **1974**, *71*, 2803.
(9) Stijve, T.; Diserens, H. In "Amanita Toxins and Poisoning"; Faulstich, H., Kommerell, B., Wieland, Th., Eds.; Witzstrock: Baden-Baden, 1980; pp 30–36.
(10) Buku, A.; Wieland, Th.; Bodenmüller, H.; Faulstich, H. *Experimentia* **1980**, *36*, 33.
(11) (a) Kostansek, E. C.; Lipscomb, W. N.; Yocum, R. R.; Thiessen, W. E. *J. Am. Chem. Soc.* **1977**, *99*, 1273; (b) *Biochemistry* **1978**, *17*, 3790.
(12) Tonelli, A. E.; Patel, D. J.; Wieland, Th.; Faulstich, H. *Biopolymers* **1978**, *17*, 1973.
(13) Wieland, Th.; Götzendörfer, C.; Zanotti, G.; Vaisius, A. C. *Eur. J. Biochem.* **1981**, *117*, 161.

0002-7863/84/1506-4606$01.50/0

Table I. Chemical Structure, Inhibition Capacity (K_i in 10^{-8} M), and Toxicity (LD_{50} in mg/kg of White Mouse) of Some Naturally Occurring (*) and Synthetic Amotoxins

name	R^1	R^2	R^3	R^4	R^5	X	LD_{50}	K_i
α-amanitin* (**1**)	NH_2	OH	OH	OH	OH	SO(*R*)	0.3	0.23
β-amanitin* (**2**)	OH	OH	OH	OH	OH	SO(*R*)	0.5	0.25
γ-amanitin* (**3**)	NH_2	OH	OH	H	OH	SO(*R*)	0.2	0.5
amanullin* (**4**)	NH_2	OH	H	H	OH	SO(*R*)	≈15	1.0
proamanullin* (**5**)	NH_2	H	H	H	OH	SO(*R*)	>20	5000
amaninamide* (**6**)	NH_2	OH	OH	OH	H	SO(*R*)	≈0.5	≈0.5
(*S*)-6′-*O*-methyl-α-amanitin (**7**)	NH_2	OH	OH	OH	OCH_3	SO(*S*)	≈15	≈2
6′-*O*-methyl-α-amanitin sulfone (**8**)	NH_2	OH	OH	OH	OCH_3	SO_2	≈1	0.57
6′-*O*-methyl-*S*-deoxo-α-amanitin (9)	NH_2	OH	OH	OH	OCH_3	S	≈0.5	0.25
S-deoxo[Ile³]amaninamide (**10**)	NH_2	OH	H	H	H	S	>50	8.1

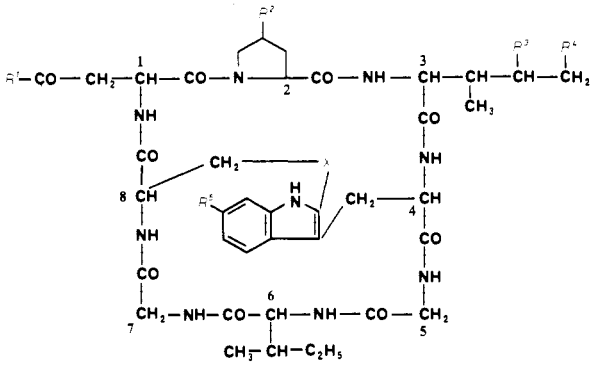

Figure 1. General chemical structure of the amatoxins. For α-amanitin, $R^1 = NH_2$, R^2 = OH, R^3, R^4 = OH, R^5 = OH, and X = S=O (*R*) (for other derivatives see Table I). Bold numbers indicate the amino acid residue numbers. For α-amanitin, 1 = Asn, 2 = hydroxyproline (HyPro), 3 = γ,δ-dihydroxyisoleucine (Dihylle), 4 = 6′-Hydroxytryptophan (HyTrp), 5 = Gly, 6 = Ile, 7 = Gly, and 8 = Cys.

In the same manner it was shown[6,13] that the γ-hydroxy group of HyPro-2, the β-methyl group of Dihylle-3, the absolute configuration of the sulfoxide bridge, and the nature of the side chains of residues 5 (Gly) and 6 (Ile) are important for the binding of amatoxins to the enzyme and for toxicity. It is not yet clear to what extent these important parts of the molecule are essential for direct binding to the enzyme, for stabilization of a certain active conformation, or for both. It is also possible that factors other than the binding affinity to the enzyme influence both inhibition and toxicity.

In an attempt to reveal the relationship between the structure and activity of amatoxins in general and the role of specific functional groups in determining the overall conformation, a series of X-ray crystallographic studies of amatoxin derivatives has been undertaken.

In an earlier paper,[14] the crystal and solution conformations of **7** and **8** were reported, indicating that there is relatively little effect of the nature of the sulfur bridge on amatoxins conformation.

In this paper we present the crystal and molecular structure of *S*-deoxo[Ile³]amaninamide (**10**), a synthetic amatoxin derivative that lacks both the γ- and δ-hydroxy groups of side chain 3 and contains a thioether sulfur bridge rather than a sulfoxide. As such, this compound serves as a good analogue for the weakly toxic natural amatoxins amanullin (**4**) and amanullinic acid (the corresponding carboxylate compound (R^1 = OH)), because of the similar nature of side chain 3, which has been shown to be very important for biological activity (Table I). The synthesis of **10** and its kinetic inhibitory parameters have been reported recently.[15] This derivative exhibits about a 30-fold reduction in binding affinity with RNA polymerase B relative to α-amanitin[13] and displays no toxicity, at least in doses up to 50 mg/kg of white mouse (Table I).

(14) Wieland, Th.; Götzendörfer, C.; Dabrowski, J.; Lipscomb, W. N.; Shoham, G. *Biochemistry*, **1983**, *22*, 1264.
(15) Zanotti, G.; Birr, C.; Wieland, Th. *Int. J. Peptide Protein Res.* **1981**, *18*, 162.

Experimental Section

Crystal Data. The crystal data were obtained using Mo Kα radiation, λ = 0.71069 Å. $C_{39}H_{54}N_{10}O_{10}S \cdot 2(C_2H_5OH) \cdot 3(H_2O)$, M = 1001.18, space group $P2_1$, a = 12.147 (1) Å, b = 11.250 (1) Å, c = 19.267 (1) Å, β = 92.41 (1)°, V = 2630.5 (3) Å³, Z = 2, D_c = 1.26 g/cm³, μ(Mo Kα) = 0.95 cm⁻¹.

Data Collection. Crystals of **10** were obtained by slow colling of a saturated solution of ethanol–water (90:10) from 80 °C to room temperature (≈20 °C). One crystal, measuring 0.70 × 0.28 × 0.22 mm, was sufficient for unit cell determination and complete data collection. The crystal had to be sealed in a glass capillary with a small amount of mother liquor in order to prevent deterioration. Systematic absences indicated that the space group is $P2_1$ (monoclinic). The unit cell parameters were calculated by least-squares fit of 25 Friedel pairs in the 2ϑ range of 17–30°.

The diffraction data were collected on an automated four-circle Nicolet R3M diffractometer with graphite monochromated Mo Kα radiation. The integrated intensities of 6525 independent reflections in the range of 3° ≤ 2ϑ ≤ 55° were measured in the ϑ/2ϑ scan mode by using variable scan speed of 3–30°/min. Corrections were applied for background, Lorentz and polarization effects and for relatively small radiation damage (decay of <5% during the 172 h of X-ray exposure). It was not necessary to make any absorption correction. Only 4097 of the measured reflections were considered to be observed ($F_o \geq \sigma(F_o)$), of which only those 3894 reflections with $F_o \geq 2.0\sigma(F_o)$ were included in further calculations.

Structure Determination. Our first attempt to solve the phase problem for **10** was a routine application of direct methods[16] which did not yield a satisfactory solution. The sulfur position could be determined from the three-dimensional Patterson function. However, due to a pseudo-centrosymmetry (one sulfur atom per asymmetric unit in space group $P2_1$ results in two heavy atoms per unit cell related by a center of symmetry), the sulfur atom was insufficient for phasing purposes. We then proceeded to molecular replacement techniques, using the known structure of **2**, **7**, and **8** as starting models, a route that eventually gave the solution of the structure.

The initial coordinated set for the structure of **10** was obtained by determining the orientation parameters required to place the known coordinates of the β-amanitin structure (**2**)[11b] in the unit cell of **10**. Evaluation of these molecular replacement parameters proceeded in two stages: (a) determination of the rotational Euler angles relating the structures of β-amanitin and **10** and (b) determination of the translation vector required to position the properly oriented β-amanitin coordinates relative to the 2_1 screw axis in the $P2_1$ unit cell of **10**.

The rotation problem was solved using Crowther's fast rotation function,[17] which calculates a product comparison of one Patterson function rotated with respect to another. Coordinates for a single β-amanitin molecule were given isotropic temperature factors of 3 Å² and placed in a $P1$ cell of dimensions $a = b = c$ = 20 Å, α = β = γ = 90°. Structure factors were calculated to 1.5-Å resolution from this model. All Fourier-transform calculations in the molecular replacement work were performed by using fast Fourier-transform programs developed by Ten Eyck.[18,19] Electron density maps were sampled at no greater than 0.5-Å intervals to ensure accurate structure factor evaluation. Structure factors used to calculate the Patterson function of β-amanitin were

(16) Main, P.; Hull, S. E.; Lessinger, L.; Germain, G.; Declercq, J. P.; Woolfson, H. M. "MULTAN-78: A System of Computer Programs for the Automatic Solution of Crystal Structures from X-ray Diffraction Data", University of York and Louvain, 1978.
(17) Crowther, R. A. In "The Molecular Replacement Method"; Rossmann, M. G., Ed.; Gordon and Breach: New York, 1972; pp 173–178.
(18) Ten Eyck, L. F. *Acta Crystallogr., Sect. A* **1973**, *A29*, 183.
(19) Ten Eyck, L. F. *Acta Crystallogr., Sect A* **1977**, *A33*, 486.

sharpened by application of an artificial temperature factor of -15 Å^2 and modified to remove the origin peak. Structure factors used to calculate the Patterson function of **10** at 1.5-Å resolution were similarly sharpened with an artificial temperature factor of -6 Å^2 and modified to remove the origin peak.

For the calculation of the rotation function, the β-amanitin Patterson function was fixed, while the Patterson function of **10** was rotated relative to it. The radius of the cutoff sphere in the Patterson function was 10 Å. The rotation function was evaluated in 2.5°, 5°, and 5° intervals of α_1, α_2, and α_3, where the α's are the three Euler angles defined by Crowther. Only one prominent peak was observed in the rotation function, with coordinates $(\alpha_1, \alpha_2, \alpha_3) = (130°, 95°, 85°)$. Since the peak width was on the order of 10°, no effort was made to sample the rotation function on a finer grid.

The matrix **Q** required to place the β-amanitin coordinates in the orientation of **10** is composed of three terms:

$$\mathbf{Q} = \mathbf{F}\cdot\mathbf{C}\cdot\mathbf{R}^{\mathrm{T}} \qquad (I)$$

R is the rotation matrix expressed in terms of the Euler angles $(\varphi, \vartheta, \psi)$.[20] As defined by Goldstein[20] $\varphi = \alpha_1 + 90°$; $\vartheta = \alpha_2$; $\psi = \alpha_3 - 90°$. The matrix **C** transforms between the orthogonal coordinate system used by Crowther (with the 2_1 screw axis along z) and an orthogonal coordinate system with the screw axis along y, and has components

$$\mathbf{C} = \begin{bmatrix} \cos\beta & \sin\beta & 0 \\ 0 & 0 & 1 \\ \sin\beta & -\cos\beta & 0 \end{bmatrix} \qquad (II)$$

where β is the monoclinic angle. **F** converts the orthogonal coordinate system used in the rotation function calculation to the crystallographic coordinate frame and has components

$$\mathbf{F} = \begin{bmatrix} 1/a & 0 & (-\cot\beta)/c \\ 0 & 1/b & 0 \\ 0 & 0 & (\csc\beta)/c \end{bmatrix} \qquad (III)$$

where β is again the monoclinic angle.

To solve the translation problem, the T_1 function of Crowther and Blow[21] was evaluated. The T_1 function essentially matches Patterson cross vectors between two test molecules related by the 2_1 screw axis with peaks in the unknown Patterson function, as a function of the displacement of the test molecule relative to the screw axis. Since the origin along the y axis in space group $P2_1$ is arbitrary, only the translational components in the x and z directions need to be determined. To evaluate the $\mathbf{T}_1$ function, structure factors to 1.5-Å resolution were calculated from a single β-amanitin molecule (with the proper rotational orientation) placed in a P 1 lattice having the cell dimensions of the unit cell of **10**. These structure factors were sharpened with an artificial temperature factor of -15 Å^2. The structure factors of **10** were also sharpened with an artificial temperature factor of -6 Å^2. The $y = {}^1/_2$ section of the T_1 function had only one large peak, located at $x = 0.833$, $z = 0.633$. Since the coordinates of this peak were related to the desired shifts by $x = -2(\Delta x)$, $z = -2(\Delta z)$, the corresponding translational shifts which placed the β-amanitin coordinates in the unit cell of **10** were $\Delta x = 0.083$, $\Delta z = 0.183$.

Although the solution of the molecular replacement problem was straightforward using the β-amanitin coordinates, attempts to determine these parameters using the coordinates of **7** and **8**[14] failed to provide a satisfactory solution. There is no apparent explanation for this behavior, since all four structures are reasonably similar to one another (see the comparison in the Discussion).

The starting model for **10** consisted of the 59 non-hydrogen atoms common to both **10** and β-amanitin and oriented according to the rotation–translation search. Least-squares refinement of the overall scale factor and isotropic thermal parameters (with fixed coordinates) of the atoms in this model, using data to 1.3-Å resolution ($2\vartheta = 3$–$32°$), resulted in an R factor of 0.43 for 1286 observations. The root mean square (rms) deviation between the atomic coordinates in this starting model and the final coordinates was later shown to be 0.76 Å (for 59 atoms; see also Figure S1 in the supplementary material).

Several cycles of difference electron density maps and least-squares refinement,[22] at increasingly higher resolution revealed the position of the

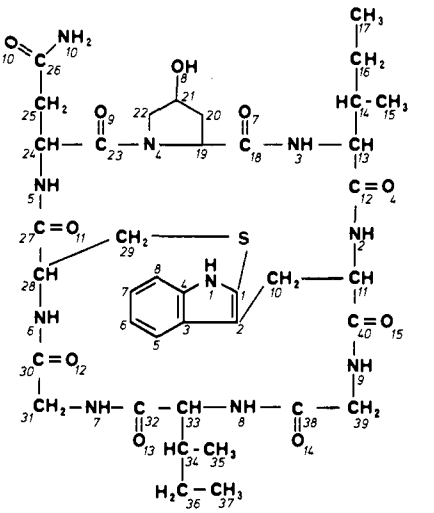

Figure 2. Chemical structure and the numbering scheme for *S*-deoxo-[Ile^3]amaninamide (**10**).

amine group, most of the hydrogen atoms of the amatoxin, and five solvent molecules (two ethanol and three water molecules). In fact, with the exception of the hydrogen atoms of side chain 3 of the cyclic peptide, all hydrogen atoms (including those of solvent molecules) were located in difference electron density maps. The side chain of residue 3 (C(14)–C(17)) and especially the terminal methyl group (C(17)) exhibited substantial disorder. C(17) was assigned four disordered positions (with statistical occupancies of 0.55, 0.20, 0.15, and 0.10) and the C(16)–C(17) distances were kept fixed during the refinement. Because of the disorder, the hydrogen atoms of this side chain could not be located in the maps. The hydrogen atoms of the terminal methyl group have not been introduced into the model, and the rest of the hydrogen atoms of this side chain have been constructed geometrically with a fixed distance from the corresponding carbon atom during refinement. One of the water molecules (W4) was assigned two disordered positions with fractional occupancies of 0.7 and 0.3.

In the final stage all non-hydrogen atom positions (except C(17)) were refined by using anisotropic temperature factors, and all the peptide hydrogen atom positions (except those mentioned above) were refined with isotropic temperature factors. The positions of solvent hydrogen atoms were kept fixed relative to the corresponding non-hydrogen atom, but most of their isotropic temperature factors were refined.

The refinement of the structure converged to values of 0.065 and 0.051 for R and R_w, respectively ($R_w = \sum(w)^{1/2}(|F_o| - |F_c|)/\sum(w)^{1/2}|F_o|$; $w = k/(\sigma^2(F_o) + |g|F_o^2)$; $k_f = 1.051$, $g_f = 0.000\,36$). In the final cycle of refinement the largest ratio of shifts to estimated standard deviations (esd's) was less than 0.2 (av 0.02), and the maximal peak in the final difference electron density map was 0.34 e/Å^3 (min, -0.29 e/Å^3).

Regarding the reliability of the final structure in light of the phasing technique used, it is noted that molecular replacement studies may suffer from the possibility of biasing the true model with the trial model. These effects are especially difficult to resolve in low-resolution studies (which are characteristic of macromolecular problems), where least-squares refinement of the model structure is poorly determined. The resolution of the present work is such, however, that a reliable least-squares refinement has been achieved. In addition, regions of the structure that differ in the molecules were omitted from the molecular replacement model, so that the initial structure would not be biased by these differences. Atoms in these regions were subsequently incorporated into the model from difference Fourier maps. Furthermore, the relatively low final R factor, the low noise level in the final difference electron density map, and the smooth, rapidly converging refinement (including most of the hydrogen atoms), are good and independent indicators for the correctness of the final structure, regardless of the technique used to solve the structure.

Results

The chemical structure and the numbering scheme of **10** are given in Figure 2. A stereoview (ORTEP[23]) of the structure is given in Figure 3. The final fractional coordinates for all non-hydrogen

(20) Goldstein, H.; "Classical Mechanics"; Addison-Wesley Press: Cambridge, MA, 1951.
(21) Crowther, R. A.; Blow, D. *Acta Crystallogr.* **1967**, *23*, 544.
(22) Sheldrick G. "Programs for Crystal Structure Determination", Cambridge, England, 1975.
(23) Johnson, C. K. "ORTEP-II, a Fortran Thermal-Ellipsoid Plot Program for Crystal Structure Illustrations", Oak Ridge National Laboratory Report ORNL-5138, 1976.

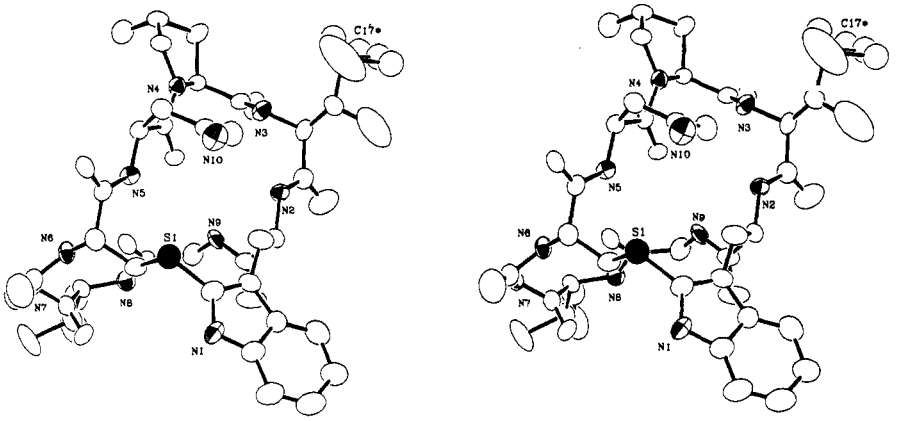

Figure 3. Stereodrawing of **10**. The four disordered positions of atom C(17) are designated by C17* (see Table II). Nitrogen atoms are indicated by partially shaded ellipsoids, and the sulfur atom is indicated by solid ellipsoid.

Table II. Positional Parameters for Non-H Atoms in the Crystal Structure of **10**

	x/a	*y/b*	*z/c*		*x/a*	*y/b*	*z/c*
S(1)	0.7037 (1)	0.2266 (1)	−0.0761 (1)	C(24)	0.6702 (4)	0.5823 (4)	−0.2105 (2)
N(2)	1.0276 (3)	0.3844 (3)	−0.2241 (2)	C(25)	0.7200 (4)	0.6311 (5)	−0.1416 (2)
C(11)	1.0060 (4)	0.2588 (4)	−0.2101 (2)	C(26)	0.8247 (3)	0.5732 (4)	−0.1177 (2)
C(10)	0.9542 (5)	0.2558 (5)	−0.1376 (2)	O(10)	0.8989 (2)	0.5544 (3)	−0.1586 (1)
C(2)	0.9135 (4)	0.1402 (4)	−0.1106 (2)	N(10)	0.8344 (5)	0.5431 (4)	−0.0523 (2)
C(1)	0.8120 (4)	0.1245 (4)	−0.0835 (2)	C(23)	0.7473 (3)	0.5906 (4)	−0.2715 (2)
C(3)	0.9717 (4)	0.0310 (4)	−0.0987 (2)	O(9)	0.7736 (2)	0.5022 (2)	−0.3039 (1)
N(1)	0.8031 (4)	0.0117 (4)	−0.0554 (2)	N(4)	0.7879 (2)	0.6981 (3)	−0.2882 (1)
C(4)	0.9011 (4)	−0.0468 (4)	−0.0635 (2)	C(19)	0.8528 (3)	0.7089 (4)	−0.3514 (2)
C(5)	1.0791 (5)	−0.0086 (6)	−0.1116 (2)	C(20)	0.8605 (5)	0.8438 (5)	−0.3624 (3)
C(8)	0.9340 (6)	−0.1607 (5)	−0.0426 (2)	C(21)	0.7553 (4)	0.8900 (4)	−0.3336 (2)
C(6)	1.1118 (6)	−0.1215 (6)	−0.0905 (3)	O(8)	0.6678 (3)	0.8650 (3)	−0.3816 (2)
C(7)	1.0388 (6)	−0.1969 (6)	−0.0570 (3)	C(22)	0.7474 (5)	0.8179 (4)	−0.2678 (2)
C(40)	0.9374 (4)	0.1976 (4)	−0.2670 (2)	C(18)	0.9627 (3)	0.6479 (4)	−0.3481 (2)
O(15)	0.9464 (3)	0.0905 (3)	−0.2757 1)	O(7)	1.0128 (2)	0.6340 (3)	−0.4029 (1)
N(9)	0.8691 (3)	0.2653 (4)	−0.3060 (2)	N(3)	1.0063 (3)	0.6158 (3)	−0.2871 (2)
C(39)	0.8172 (4)	0.2256 (6)	−0.3701 (2)	C(12)	1.1016 (3)	0.4218 (4)	−0.2684 (2)
C(38)	0.6923 (3)	0.2215 (4)	−0.3712 (2)	O(4)	1.575 (3)	0.3524 (3)	−0.2999 (2)
O(14)	0.6376 (2)	0.2679 (3)	−0.3261 (1)	C(13)	1.1132 (4)	0.5568 (4)	−0.2770 (2)
N(8)	0.6459 (3)	0.1632 (3)	−0.4263 (2)	C(14)	1.1806 (4)	0.6159 (5)	−0.2163 (3)
C(33)	0.5271 (3)	0.1486 (4)	−0.4966 (2)	C(15)	1.2648 (7)	0.5417 (11)	−0.1847 (6)
C(34)	0.5054 (4)	0.0618 (5)	−0.4998 (2)	C(16)	1.2219 (8)	0.7400 (8)	−0.2424 (4)
C(36)	0.5288 (5)	0.1227 (6)	−0.5688 (3)	C(17)[a]	1.2730 (8)	0.7630 (8)	−0.3020 (4)
C(35)	0.3870 (6)	0.0120 (9)	−0.5018 (4)	C(171)	1.2060 (8)	0.8050 (8)	−0.2980 (4)
C(37)	0.5292 (8)	0.0347 (11)	−0.6295 (4)	C(172)	1.3200 (8)	0.7450 (8)	−0.2890 (4)
C(32)	0.4748 (3)	0.1066 (4)	−0.3723 (2)	C(173)	1.3450 (8)	0.7230 (8)	−0.2620 (4)
O(13)	0.5105 (2)	0.0211 (3)	−0.3383 (1)	O(E1)[b]	0.8926 (3)	0.6467 (4)	−0.5275 (2)
N(7)	0.3852 (3)	0.1673 (3)	−0.3542 (2)	C1(E1)	0.9046 (6)	0.5412 (7)	−0.5677 (3)
C(31)	0.3265 (4)	0.1358 (5)	−0.2924 (2)	C2(E1)	0.8989 (6)	0.4340 (8)	−0.5247 (4)
C(30)	0.3747 (4)	0.1859 (4)	−0.2245 (2)	O(E2)	0.4095 (3)	0.4173 (3)	−0.0029 (2)
O(12)	0.3314 (3)	0.1591 (4)	−0.1708 (1)	C1(E2)	0.5052 (7)	0.4402 (9)	0.0463 (4)
N(6)	0.4647 (3)	0.2551 (3)	−0.2281 (2)	C2(E2)	0.4993 (8)	0.3729 (10)	0.1085 (5)
C(28)	0.5322 (4)	0.2858 (4)	−0.1663 (2)	O(W2)	0.3086 (4)	0.1890 (4)	−0.0308 (2)
C(29)	0.6318 (4)	0.2033 (5)	−0.1597 (2)	O(W3)	0.8043 (3)	0.0564 (4)	−0.5159 (2)
C(27)	0.5600 (3)	0.4188 (4)	−0.1639 (2)	O(W4)	0.2353 (3)	0.3302 (4)	−0.4274 (2)
O(11)	0.5119 (2)	0.4872 (3)	−0.1249 (1)	O(W41)[c]	0.2790 (3)	0.3190 (4)	−0.4710 (2)
N(5)	0.6379 (3)	0.4575 (3)	−0.2058 (1)				

[a] C(17)–C(173) are the four disordered positions of C(17) with partial occupancies of 0.55, 0.20, 0.15, and 0.10, respectively. [b] E1–W3 are the five solvent molecules (E ethanol, W water). [c] O(W4) and O(W41) are the two disordered positions of W4 (with occupancies of 0.7 and 0.3).

atoms in the crystal structure are listed in Table II. The anisotropic temperature parameters are listed in Table III. Bond lengths and bond angles in the structure, together with their esd's, are listed in Table IV and V, respectively.[24] Coordinates and temperature parameters of all hydrogen atoms, bond lengths involving hydrogen atoms, and torsion angles of the peptide are given in the supplementary material.

Molecular Structure. The overall structure of the cyclic peptide **10** is relatively similar to the structures of β-amanitin[11] and the amatoxin derivatives **7** and **8**.[14] The large macrocyclic octapeptide ring of 24 atoms is "bent" at the bridging points. The bridging segment of five atoms (containing the indole ring and the thioether group) participates in two 18-membered rings (designated ring 1 and ring 2) both of which display a fairly "flat" conformation, often observed in 18-membered rings of cyclohexapeptides. Ring 1 contains the backbone of residues 1, 2, and 3 (N(2)–N(5) in Figure 3), and ring 2 contains the backbone of residues 5, 6, and 7 (N(6)–N(9) in Figure 3). The planes of these two rings form a dihedral angle of about 80°. The indole ring lies approximately in the "plane" of ring 1 giving the molecule an overall distorted "T" shape. In comparison to β-amanitin[11] ring 1 (or the cross bar of the T) is much less hydrophilic, lacking three hydroxyl, carboxyl, and sulfoxide groups, yet still significantly more hydrophilic than ring 2 (or the stem of the T).

(24) One of the referees pointed out that the esd's of coordinates, bond lengths, and bond angles in disordered parts of the molecule could be severely underestimated by standard least-squares techniques.

Table III. Anisotropic Temperature Factors ($\times 10^3$) in the Form

$$e^{[-2\pi^2(U_{11}h^2a^{*2} + U_{22}k^2b^{*2} + U_{33}l^2c^{*2} + 2U_{23}klb^*c^* + 2U_{13}lhc^*a^* + 2U_{12}hka^*b^*)]}$$

	U_{11}	U_{22}	U_{33}	U_{23}	U_{13}	U_{12}
S(1)	55 (1)	60 (1)	41 (1)	0 (1)	−3 (1)	14 (1)
N(2)	39 (2)	27 (2)	46 (2)	−1 (2)	9 (2)	10 (2)
C(11)	37 (3)	36 (3)	41 (3)	−3 (2)	5 (2)	5 (3)
C(10)	64 (4)	40 (3)	39 (3)	−8 (3)	−4 (3)	−6 (3)
C(2)	47 (3)	37 (3)	30 (3)	−4 (2)	−6 (2)	−2 (3)
C(1)	48 (3)	40 (3)	36 (3)	5 (2)	−4 (2)	6 (3)
C(3)	47 (3)	43 (3)	34 (3)	−2 (2)	−5 (2)	1 (3)
N(1)	45 (3)	52 (3)	55 (3)	16 (2)	1 (2)	1 (3)
C(4)	59 (4)	46 (3)	31 (3)	2 (2)	−11 (3)	1 (3)
C(5)	59 (4)	62 (4)	44 (3)	−10 (3)	9 (3)	4 (4)
C(6)	94 (5)	42 (4)	39 (3)	15 (3)	−19 (3)	−5 (4)
C(6)	77 (5)	60 (5)	56 (4)	−3 (3)	−3 (4)	23 (4)
C(7)	96 (6)	54 (4)	53 (4)	0 (3)	−19 (4)	27 (4)
C(40)	48 (3)	37 (3)	34 (3)	−2 (2)	3 (2)	10 (3)
O(15)	113 (3)	35 (2)	57 (2)	−8 (2)	−19 (2)	11 (2)
N(9)	37 (3)	39 (3)	49 (3)	−5 (2)	−8 (2)	−4 (2)
C(39)	39 (3)	56 (4)	38 (3)	5 (3)	−1 (2)	−3 (3)
C(38)	34 (3)	31 (3)	40 (3)	0 (3)	1 (2)	−1 (3)
O(14)	36 (2)	46 (2)	42 (2)	−10 (2)	6 (2)	−2 (2)
N(8)	34 (3)	47 (3)	45 (3)	−4 (2)	11 (2)	5 (2)
C(33)	30 (3)	38 (3)	46 (3)	−8 (3)	3 (2)	8 (3)
C(34)	37 (3)	58 (4)	45 (3)	−6 (3)	−1 (2)	8 (3)
C(36)	57 (4)	75 (5)	56 (4)	−6 (3)	−8 (3)	0 (4)
C(35)	57 (5)	109 (7)	78 (5)	−31 (6)	−6 (4)	−25 (5)
C(37)	64 (7)	149 (9)	59 (5)	−33 (6)	6 (4)	−17 (7)
C(32)	32 (3)	38 (3)	39 (3)	−2 (3)	−1 (2)	−4 (3)
O(13)	41 (2)	46 (2)	64 (2)	11 (2)	8 (2)	14 (2)
N(7)	34 (3)	39 (3)	42 (3)	−3 (2)	4 (2)	8 (2)
C(31)	34 (3)	45 (4)	46 (3)	−11 (3)	3 (2)	1 (3)
C(30)	37 (3)	41 (3)	55 (3)	−2 (3)	5 (3)	−5 (3)
O(12)	74 (3)	113 (4)	47 (2)	−4 (2)	14 (2)	−55 (3)
N(6)	34 (2)	46 (3)	27 (2)	2 (2)	4 (2)	−6 (2)
C(28)	40 (3)	50 (3)	26 (3)	0 (2)	12 (2)	1 (3)
C(29)	51 (3)	36 (3)	40 (3)	2 (3)	−2 (3)	4 (3)
C(27)	31 (3)	43 (3)	34 (3)	3 (2)	6 (2)	−2 (3)
O(11)	36 (2)	57 (2)	56 (2)	−9 (2)	20 (2)	1 (2)
N(5)	41 (2)	34 (2)	30 (2)	0 (2)	9 (2)	0 (2)
C(24)	38 (3)	30 (3)	35 (3)	0 (2)	8 (2)	7 (2)
C(25)	43 (3)	39 (3)	36 (3)	−5 (3)	12 (3)	5 (3)
C(26)	40 (3)	30 (3)	32 (3)	−2 (2)	3 (2)	3 (2)
O(10)	51 (2)	60 (2)	40 (2)	−2 (2)	10 (2)	17 (2)
N(10)	66 (4)	65 (4)	39 (3)	1 (3)	−2 (3)	13 (3)
C(23)	29 (3)	29 (3)	29 (2)	4 (2)	5 (2)	0 (2)
O(9)	40 (2)	28 (2)	45 (2)	−1 (2)	10 (2)	4 (2)
N(4)	33 (2)	30 (2)	36 (2)	1 (2)	9 (2)	4 (2)
C(19)	33 (3)	31 (3)	40 (3)	2 (3)	6 (2)	3 (2)
C(20)	51 (4)	40 (3)	59 (4)	13 (3)	11 (3)	7 (3)
C(21)	40 (3)	29 (3)	67 (4)	−2 (3)	7 (3)	5 (3)
O(8)	53 (3)	57 (3)	66 (3)	2 (2)	0 (2)	28 (2)
C(22)	49 (4)	25 (3)	56 (4)	−2 (3)	14 (3)	11 (3)
C(18)	38 (3)	32 (3)	41 (3)	2 (2)	8 (2)	3 (2)
O(7)	51 (2)	78 (3)	43 (2)	5 (2)	12 (2)	24 (2)
N(3)	37 (2)	40 (3)	38 (2)	9 (2)	18 (2)	7 (2)
C(12)	34 (3)	48 (3)	39 (3)	0 (3)	−1 (2)	12 (3)
O(4)	86 (3)	59 (3)	78 (3)	17 (2)	44 (2)	40 (3)
C(13)	37 (3)	44 (3)	45 (3)	8 (3)	8 (3)	7 (3)
C(14)	41 (3)	58 (4)	93 (5)	−4 (4)	−9 (3)	−7 (3)
C(15)	166 (10)	168 (11)	327 (16)	−75 (12)	−195 (11)	41 (10)
C(16)	188 (11)	241 (14)	143 (9)	−118 (9)	67 (8)	−144 (11)
O(E1)	100 (4)	84 (3)	75 (3)	−8 (3)	−17 (3)	39 (3)
C1(E1)	76 (5)	111 (6)	72 (4)	9 (5)	19 (4)	29 (5)
C2(E1)	87 (6)	88 (6)	154 (8)	38 (6)	29 (5)	24 (5)
O(E2)	75 (3)	81 (3)	69 (3)	−13 (2)	26 (3)	−9 (3)
C1(E2)	125 (8)	106 (7)	103 (7)	−9 (6)	14 (6)	−15 (6)
C2(E2)	188 (10)	159 (10)	140 (9)	42 (8)	−44 (9)	−38 (9)
O(W2)	131 (4)	103 (4)	54 (3)	−5 (3)	37 (3)	−33 (3)
O(W3)	60 (3)	70 (3)	82 (3)	−25 (2)	37 (2)	−14 (2)
O(W4)	59 (3)	55 (3)	38 (3)	−2 (3)	−3 (3)	0 (3)

The backbone bond lengths and angles are similar to those usually found in polypeptide structures. The average values for backbone bond lengths are 1.46, 1.52, 1.23, and 1.34 Å (Table IV) for N_i–C_i^α, C_i^α–C_i, C_i–O_i and C_i–N_{i+1}, respectively. The average values for backbone bond angles are 122°, 112°, 117°, 121°, and 122° (Table V) for C_{i-1}–N_i–C_i^α, N_i–C_i^α–C_i, C_i^α–C_i–N_{i+1}, C_i^α–C_i–O_i, and O_i–C_i–N_{i+1}, respectively. These values agree rather well with weighted average results of polypeptide structures,[25,26] which are 1.45, 1.52, 1.23, and 1.33 Å for the corresponding distances and 122°, 111°, 116°, 120.5°, and

Table IV. Bond Lengths (Å)

C(1)–S(1)	1.756 (5)	C(29)–S(1)	1.819 (5)
C(11)–N(2)	1.465 (6)	C(12)–N(2)	1.334 (6)
C(10)–C(11)	1.555 (7)	C(40)–C(11)	1.515 (7)
C(2)–C(10)	1.492 (8)	C(1)–C(2)	1.371 (7)
C(3)–C(2)	1.431 (7)	N(1)–C(1)	1.386 (7)
C(4)–C(3)	1.418 (7)	C(5)–C(3)	1.410 (8)
C(4)–N(1)	1.375 (7)	C(8)–C(4)	1.396 (8)
C(6)–C(5)	1.386 (10)	C(7)–C(8)	1.376 (11)
C(7)–C(6)	1.404 (10)	O(15)–C(40)	1.222 (6)
N(9)–C(40)	1.333 (6)	C(39)–N(9)	1.434 (7)
C(38)–C(39)	1.518 (7)	O(14)–C(38)	1.232 (6)
N(8)–C(38)	1.350 (6)	C(33)–N(8)	1.462 (6)
C(34)–C(33)	1.546 (8)	C(32)–C(33)	1.525 (7)
C(36)–C(34)	1.532 (8)	C(35)–C(34)	1.542 (10)
C(37)–C(36)	1.532 (12)	O(13)–C(32)	1.232 (6)
N(7)–C(32)	1.343 (7)	C(31)–N(7)	1.458 (7)
C(30)–C(31)	1.519 (7)	O(12)–C(30)	1.219 (6)
N(6)–C(30)	1.346 (6)	C(28)–N(6)	1.458 (6)
C(29)–C(28)	1.526 (8)	C(27)–C(28)	1.533 (7)
O(11)–C(27)	1.239 (6)	N(5)–C(27)	1.341 (6)
C(24)–N(5)	1.463 (6)	C(25)–C(24)	1.538 (7)
C(23)–C(24)	1.535 (6)	C(26)–C(25)	1.485 (7)
O(10)–C(26)	1.241 (6)	N(10)–C(26)	1.305 (7)
O(9)–C(23)	1.224 (6)	N(4)–C(23)	1.349 (6)
C(19)–N(4)	1.483 (6)	C(22)–N(4)	1.493 (6)
C(20)–C(19)	1.535 (7)	C(18)–C(19)	1.501 (7)
C(21)–C(20)	1.508 (8)	O(8)–C(21)	1.408 (7)
C(22)–C(21)	1.511 (8)	O(7)–C(18)	1.249 (6)
N(3)–C(18)	1.320 (6)	C(13)–N(3)	1.463 (6)
C(14)–C(13)	1.550 (8)	C(12)–C(13)	1.534 (7)
C(15)–C(14)	1.435 (13)	C(16)–C(14)	1.572 (11)
O(4)–C(12)	1.213 (6)	C1(E1)–O(E1)	1.428 (9)
C2(E1)–C1(E1)	1.466 (12)	C1(E2)–O(E2)	1.491 (10)
C2(E2)–C1(E2)	1.423 (14)		

Table V. Bond Angles (deg)

C(29)–S(1)–C(1)	99.7 (2)	C(12)–N(2)–C(11)	123.6 (4)
C(10)–C(11)–N(2)	105.6 (4)	C(40)–C(11)–N(2)	113.7 (4)
C(40)–C(11)–C(10)	114.2 (4)	C(2)–C(10)–C(11)	119.1 (4)
C(1)–C(2)–C(10)	124.2 (5)	C(3)–C(2)–C(10)	129.3 (5)
C(3)–C(2)–C(1)	106.0 (4)	C(2)–C(1)–S(1)	129.5 (4)
N(1)–C(1)–S(1)	119.8 (4)	N(1)–C(1)–C(2)	110.7 (4)
C(4)–C(3)–C(2)	107.5 (4)	C(5)–C(3)–C(2)	134.3 (5)
C(5)–C(3)–C(4)	118.1 (5)	C(4)–N(1)–C(1)	108.2 (4)
N(1)–C(4)–C(3)	107.7 (4)	C(8)–C(4)–C(3)	122.2 (5)
C(8)–C(4)–N(1)	130.2 (5)	C(6)–C(5)–C(3)	119.7 (6)
C(7)–C(8)–C(4)	118.0 (6)	C(7)—C(6)–C(5)	120.6 (7)
C(6)–C(7)–C(8)	121.4 (6)	O(15)–C(40)–C(11)	119.8 (4)
N(9)–C(40)–C(11)	117.3 (4)	N(9)–C(40)–O(15)	122.9 (5)
C(39)–N(9)–C(40)	123.2 (5)	C(38)–C(39)–N(9)	115.1 (4)
O(14)–C(38)–C(39)	123.0 (4)	N(8)–C(38)–C(39)	114.3 (4)
N(8)–C(38)–O(14)	122.7 (4)	C(33)–N(8)–C(38)	124.0 (4)
C(34)–C(33)–N(8)	109.3 (4)	C(32)–C(33)–N(8)	110.0 (4)
C(32)–C(33)–C(34)	112.3 (4)	C(36)–C(34)–C(33)	110.3 (5)
C(35)–C(34)–C(33)	112.2 (5)	C(35)–C(34)–C(36)	110.4 (5)
C(37)–C(36)–C(34)	112.3 (6)	O(13)–C(32)–C(33)	122.5 (4)
N(7)–C(32)–C(33)	115.5 (4)	N(7)–C(32)–O(13)	122.0 (4)
C(31)–N(7)–C(32)	121.2 (4)	C(30)–C(31)–N(7)	115.4 (4)
O(12)–C(30)–C(31)	118.4 (5)	N(6)–C(30)–C(31)	117.1 (4)
N(6)–C(30)–O(12)	124.5 (5)	C(28)–N(6)–C(30)	121.7 (4)
C(29)–C(28)–N(6)	109.9 (4)	C(27)–C(28)–N(6)	111.8 (4)
C(27)–C(28)–C(29)	114.7 (4)	C(28)–C(29)–S(1)	109.6 (4)
O(11)–C(27)–C(28)	121.0 (4)	N(5)–C(27)–C(28)	117.3 (4)
N(5)–C(27)–O(11)	121.7 (5)	C(24)–N(5)–C(27)	123.2 (4)
C(25)–C(24)–N(5)	112.6 (4)	C(23)–C(24)–N(5)	106.3 (4)
C(23)–C(24)–C(25)	114.1 (4)	C(26)–C(25)–C(24)	114.3 (4)
O(10)–C(26)–C(25)	120.9 (4)	N(10)–C(26)–C(25)	117.0 (5)
N(10)–C(26)–O(10)	122.1 (5)	O(9)–C(23)–C(24)	121.4 (4)
N(4)–C(23)–C(24)	118.6 (4)	N(4)–C(23)–O(9)	120.0 (4)
C(19)–N(4)–C(23)	118.8 (4)	C(22)–N(4)–C(23)	128.2 (4)
C(22)–N(4)–C(19)	109.5 (4)	C(20)–C(19)–N(4)	103.5 (4)
C(18)–C(19)–N(4)	115.5 (4)	C(18)–C(19)–C(20)	113.5 (4)
C(21)–C(20)–C(19)	103.4 (5)	O(8)–C(21)–C(20)	108.5 (5)
C(22)–C(21)–C(20)	102.1 (5)	C(22)–C(21)–O(8)	111.8 (4)
C(21)–C(22)–N(4)	103.3 (4)	O(7)–C(18)–C(19)	119.0 (4)
N(3)–C(18)–C(19)	119.1 (4)	N(3)–C(18)–O(7)	121.8 (4)
C(13)–N(3)–C(18)	124.3 (4)	C(14)–C(13)–N(3)	110.1 (4)
C(12)–C(13)–N(3)	112.2 (4)	C(12)–C(13)–C(14)	113.1 (4)
C(15)–C(14)–C(13)	114.5 (7)	C(16)–C(14)–C(13)	107.8 (5)
C(16)–C(14)–C(15)	114.9 (7)	C(13)–C(12)–N(2)	116.6 (4)
O(4)–C(12)–N(2)	121.5 (5)	O(4)–C(12)–C(13)	121.9 (5)
C2(E1)–C1(E1)–O(E1)	111.7 (8)	C2(E2)–C1(E2)–O(E2)	112.2 (8)

123° for the corresponding angles.

The peptide-backbone conformational angles (see supplementary material) fall generally into the allowed regions of a Ramachandran plot.[27] The specific torsion angles and comparison with the corresponding angles (φ and ψ) in the other amatoxin structures are discussed elsewhere.[28]

All the peptide bonds are generally in the trans conformation. Six out of eight peptide bonds deviate by less than 7° from the ideal trans conformation (ω = 180°), while the two peptide bonds between residues 4 and 5 and between residues 7 and 8 (torsion angles C(11)–C(40)–N(9)–C(39) and C(31)–C(30)–N(6)–C(28), respectively, deviate from ideal trans conformation by about 14°. The deviation of these two peptide bonds from the trans conformation suggests that a small amount of strain is present around the bridging points, distorting to a small extent the peptide bonds between the bridging residues and the adjacent and more flexible glycine residues. However, all the above data indicate principally that the peptide backbone is not experiencing a large strain due to the bicyclic frame or the compact intramolecular interactions.

Bond lengths, bond angles, and conformations in the peptide side chains agree in general with the corresponding parameters compiled from small molecules[29] or proteins.[30,31] A more specific comparison with Tables IV and V and the examination of the peptide torsion angles shows some deivations worth detailing, however. In the asparagine side chain (residue 1) the C(25)–C(26) bond (1.48 Å) and the C(26)–N(10) bond (1.30 Å) are somewhat shorter than usual.[29] The torsion angle N(5)–C(24)–C(25)–C(26) of 63° is similar to the corresponding angle in the isolated amino acid,[32] but such a conformation is the least common in proteins.[30] The amide group is tilted by 45° from the side-chain plane, unlike the parallel orientation in the isolated amino acid.[32] A molecular model based on our crystal structure indicates that the conformational values for this side chain are rather limited to the observed ones because of the close intramolecular Van der Waals interaction in this region and the two intramolecular hydrogen bonds, in which the terminal amide oxygen O(10) participates (Figures 3 and 4).

In the proline ring of side chain 2, four atoms are nearly coplanar and the C^{γ} atom (C(21)) is displaced from the plane by ≈0.5 Å as is commonly observed.[25a,26,33] The C^{γ} displacement is away from the carbonyl group (to the left in Figure 3) and so is the direction of the γ-substituted hydroxyl group, resulting in an *R* configuration at C^{γ}. This conformation is defined as C_S–C^{γ}–exo[33] or "up"[29] and is similar to that in the β-amanitin structure[11] and in the structure of the isolated hydroxyproline molecule.[34]

(25) (a) Marsh, R. E.; Donohue, J. *Adv. Protein Chem.* **1967**, *22*, 235. (b) Ramachandran, G. N.; Kolaskar, A. A.; Ramakrishnan, C.; Sasisekharan, V. *Biochim. Biophys. Acta* **1974**, *359*, 298.

(26) Benedetti, E. In "Peptides"; Goodman, M., Meienhofer, J., Eds.; Wiley: New York, 1977; pp 257.

(27) Ramachandran, G. N.; Ramakrishnan, C.; Sasisekharan, V. *J. Mol. Biol.* **1963**, *7*, 95.

(28) Shoham, G.; Lipscomb, W. N.; Wieland, Th., in press.

(29) Momany, F. A.; McGuire, R. F.; Burgess, A. W.; Scheraga, H. A. *J. Phys. Chem.* **1975**, *79*, 2361.

(30) Bhat, T. N.; Sasisekharan, V.; Vijayan, M. *Int. J. Peptide Protein Res.* **1979**, *13*, 170.

(31) Janin, J.; Wodak, S.; Levitt, M., Maigret, B. *J. Mol. Biol.* **1978**, *125*, 357.

(32) Ramanadham, M.; Sikka, S. K.; Chidambaram, R. *Acta Crystallogr., Sect. B* **1972**, *B28*, 3000.

(33) Ashida, T.; Kakudo, M. *Bull. Chem. Soc. Jpn.* **1974**, *47*, 1129.

(34) Koetzle, T. F.; Lehmann, M. S.; Hamilton, W. C. *Acta Crystallogr., Sect. B* **1973**, *B29*, 231.

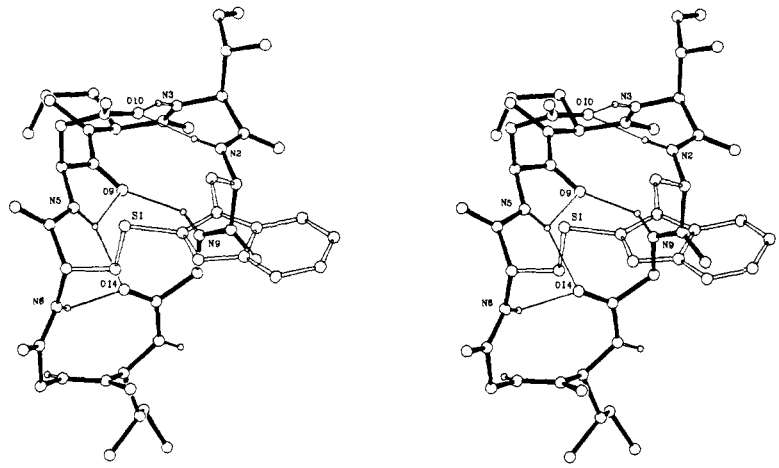

Figure 4. Intramolecular hydrogen bonds (thin lines) in the structure of **10**. The primary 24-membered cyclic peptide is emphasized (solid lines) while the sulfur bridge is kept "transparent" (double lines) for clarity.

In isoleucine residue 3, atoms $C^{\gamma 2}$ (C(15)) and $C^{\gamma 1}$ (C(16)) display relatively large thermal parameters (Table III), and atom C^{δ} (C(17)) is disordered, and its position is statistically distributed among four partially occupied sites (Table II). Bond lengths involving these three atoms significantly deviate from the standard values,[29] probably due to thermal motion and disorder. However, the corresponding bond angles compare well with the accepted values.[29] The torsion angles described by N(3)–C(13–C(14)–C-(15) and N(3)–C(13)–C(14)–C(16) measure 157° and -73°, respectively, values that are similar to those of the "normal" isoleucine side chain 6 and compare favorably with the corresponding gauche and trans conformations reported for the isolated amino acid[35] and those observed for isoleucine residues in protein structures.[30] The torsion angle described by C(13)–C(14)–C-(16)–C(17) is not well defined in our structure because of the disorder of C(17).

All the above data suggest that there is a slight rotational freedom around the C(13)–C(14) bond (see also the direction of the thermal ellipsoids of C(15) and C(16) in Figure 3) and partial rotation around the C(14)–C(16) bond in the crystal structure of **10**.

The indole ring of the tryptophan residue is very nearly planar, as expected, and its structural parameters are similar to those in nonbridging indole structures[25a,29] and the structure of the isolated amino acid.[36] However, the conformation torsion angles N-(2)–C(11)–C(10)–C(2) and C(11)–C(10)–C(2)–C(1) of 175° (nearly trans) and -131°, respectively, are, not surprisingly, different from the more commonly observed values of -60° and 90° in proteins or 60° and 90° in small molecules.[36] This deviation from a common and more stable conformation is probably due to the bridging effect and the bulk of the indole ring. For the same reason, the cysteine side chain (the other side of the bridge) is "forced" into an uncommon[31,37] conformational angle (N(6)–C(28)–C(29)–S(1) of 127°.

The bridging thioether group differs in chemical nature from the bridging sulfur groups of β-amanitin and derivatives **7** and **8** ((*R*)-sulfoxide, (*S*)-sulfoxide, and sulfone, respectively; Table I), yet the C(1)–S–C(29) group geometry is relatively similar in all four structures.[28] The C(29)–S distance of 1.82 Å is longer by 0.03–0.07 Å than the analogous distance in the other three derivatives but agrees well with the usual C–S bond distances[38] and the C–S bond distance in cysteine structures.[29,37]

A final note on the molecular structure is that all asymmetric carbon atoms possess the same absolute configurations as those of the corresponding centers in the structure of β-amanitin.[11]

Table VI. Hydrogen Bonds (Intramolecular and Intermolecular) of Less Than 3.2 Å (std deviation is <0.01 Å) in the Crystal Structure of **10** (See Figure 4)

a. Intramolecular Hydrogen Bonds			
N(2)–H···O(10)	2.80	N(5)–H···O(14)	3.15
N(3)–H···O(10)	2.93	N(6)–H···O(14)	2.89
N(5)–H[a]···O(9)	2.61	N(9)—H···O(9)	2.91
b. Intermolecular Hydrogen Bonds			
Peptide–Peptide			
O(8)–H···O(13)′	2.75		
Peptide–Solvent			
N(1)–H···O(E2)′	3.05	O(E1)–H···O(7)	2.76
N(7)–H···O(W4)	2.91	O(W3)″H(1)···O(7)	2.91
N(8)–H···O(W3)	2.90	O(E2)–H···O(11)	2.82
N(10)–H(0)···O(W2)′	2.92	O(W2)–H(1)···O(12)	2.74
Solvent–Solvent			
O(W2)–H(2)···O(E2)	2.89	O(W4)′–H(1)···O(E1)	2.70
O(W3)′–H(2)···O(W4)	2.80		

[a] 2→2 H bond, H–(N(5))···O(9) is 2.16 Å.

Intramolecular Hydrogen Bonds. Five backbone N–H groups (N(2), N(3), N(5), N(6), and N(9)) and two backbone carbonyl groups (O(9) and O(14)) are directed toward the interior of the cyclopeptide. Together with the carbonyl of Asn(1) side chain (O(10)), these eight groups construct a rather extensive intramolecular hydrogen-bonding system among themselves, holding the bicyclic frame in a relatively tight and rigid conformation. There are six intramolecular hydrogen bonds (Table VIa and Figure 4), three of which are transannular (across the peptide primary 24-membered macrocycle). Two of these transannular H bonds, a 4→1 trans (2) H bond (or β-turn)[39-41] between N(6) and O(14) and a weak 5→1 (all trans) H bond (or α-turn)[40,41] between N(5) and O(14), stabilize one of the turns of the peptide ring. The third transannular H bond, a 5→1 (all trans) H bond between N(9) and O(9), stabilizes the other peptide turn. This turn is additionally reinforced by two backbone to side-chain interactions, H bonds between N(2) and O(10) and between N(3) and O(10) (Figure 4). Furthermore, a 2→2 (or C_5) H bond[40] between N(5) and O(9) (resulting in a bifurcated H bond at N(5)) connects the two hydrogen-bonded turns and yields additional overall conformational rigidity. The 2→2 H bond has been shown to be a real, although weak, intramolecular interaction,[40] and several experimental examples have been reported.[41] In a typical 2→2 H bond, as in our case, the peptide backbone is fully extended and the N···O and H···O distances measure approximately 2.6 and 2.15 Å, respectively.[40]

(35) Torii, K.; Iitaka, Y. *Acta Crystallogr., Sect. B* **1971**, *B27*, 2237.
(36) Takigawa, T.; Ashida, T.; Sasada, Y.; Kakudo, M. *Bull. Chem. Soc. Jpn.* **1966**, *39*, 2369.
(37) Kerr, K. A.; Ashmore, J. P. *Acta Crystallogr., Sect. B* **1973**, *B29*, 2124.
(38) "International Tables for X-ray Crystallography": Reidel: Dordrecht, Holland, 1983; Vol. III, p 276.
(39) Venkatachalam, C. M. *Biopolymers* **1968**, *6*, 1425.
(40) Toniolo, C. In "Bioorganic Chemistry"; van Tamelen, E. E. Ed.; Academic Press: New York, 1977; Vol. 3, pp 265–291.
(41) Toniolo, C. *CRC Crit. Rev. Biochem.* **1980**, *9*, 1 and references therein.

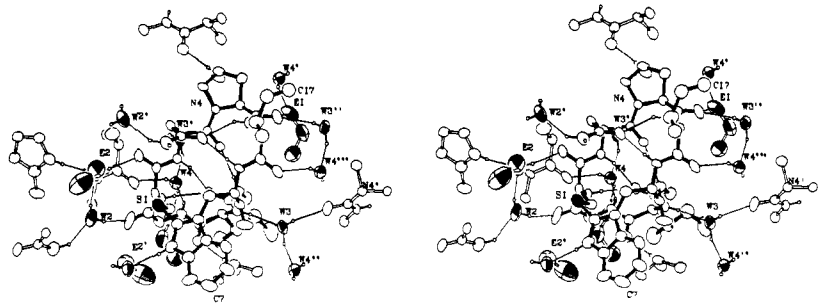

Figure 5. Solvent molecules and hydrogen-bonding system in the crystal structure of **10**. Cyclopeptide **10** is outlined by the solid lines. Interacting regions of neighboring peptide molecules are represented by double lines. Hydrogen bonds are indicated by thin lines. The non-hydrogen atoms of the solvent molecules are represented by shaded ellipsoids.

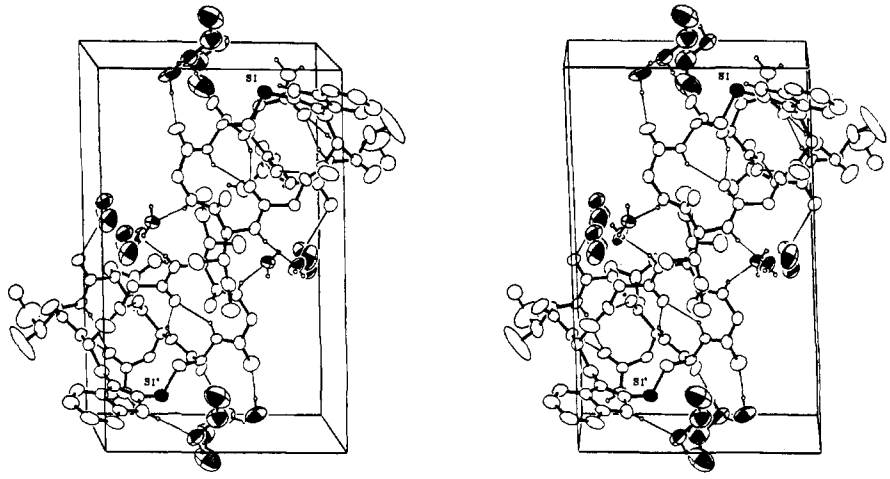

Figure 6. Stereodrawing of the unit cell packing of **10**, viewed down the 2_1 axis ($c \uparrow$, $a \rightarrow$). Solvent molecules are represented by shaded ellipsoids.

Except for the 2→2 H bond and the N(5)–O(14) H bond, the other four intramolecular H bonds are rather strong. The N–H···O distances of 2.80–2.93 Å (Table VI) are relatively shorter than the usually observed range of 2.9–3.0 Å.[42]

Intermolecular Interactions. An interesting and complicated intermolecular hydrogen-bonding scheme in the crystal structure of **10** is presented in Figure 5 and Table VI. The analysis of this type of interaction is important since it might provide some insight to the nature of interactions between amatoxins and their binding sites on RNA polymerase B.

The intermolecular H-bonding scheme consists of peptide–peptide, peptide–solvent, and solvent–solvent interactions. A strong H bond between the δ-hydroxy group (O(8)) of the hydroxyproline residue and the backbone carbonyl group O(13) directly connects neighboring cyclopeptides. Additional bridges between adjacent cyclopeptides are provided by the solvent molecules. There are two ethanol molecules (E1 and E2) and three water molecules (W2, W3, and W4) in each asymmetric unit of the crystal. Except for one of the water molecules, W4, which appears to occupy statistically two positions (Table II), the solvent molecules are well defined.

Two backbone N–H groups (N(7) and (N8)) and two side-chain N–H groups (N(1) and N(10)) are H bonded to the oxygen atom of a solvent molecule (O(W4), O(W3), O(E2), and O(W2), respectively). Three backbone carbonyl groups (O(4), O(11), and O(12)) are H bonded with a solvent molecule O–H groups (O(W4), O(E2), and O(W2), respectively), whereas another backbone carbonyl group (O(7)) forms two H bonds with the O–H groups of E1 and W3 (Figure 5).

The solvent molecules are further interconnected among themselves by H bonds between the O–H groups of W2, W3, and W4, and the oxygen atoms of E2, W4, and E1, respectively (Table VIb). The resulting "network" of H bonds provides two intramolecular "solvent-bridges" and four intermolecular "solvent-bridges". The intramolecular bridges are made of the H-bonded sequences of O(7)←W3→W4→O(4) and O(12)←W2→E2→O(11), where "→" designates the direction of the H bond, offering further support to an already firm molecular conformation. The intermolecular bridges are made of the H-bond sequences of N(1)→E2→O(11)′, N(7)→W4→O(4)′, N(7)→W4→E1→O(7)′, N(8)→W3→O(7)′, and N(10)→W2→O(12).

All of the intermolecular H bonds are rather strong (interaction distances of 2.68–3.05 Å, av 2.83 Å) in comparison to those commonly observed.[42,43] It is interesting to note that except for one backbone carbonyl group (O(15)) and one of the side-chain amide hydrogens (on N(10)), all of the potentially hydrogen-bond-forming groups are involved in one or more H bonds.

Crystal Packing. Figure 6 presents a stereoview of the crystal unit cell, looking down the crystallographic 2_1 axis. The two cyclic peptides, related by the 2_1 axis, form a hydrophobic interior, defined by the two neighboring isoleucine (residues 6 and 6′) side chains, located at the center of the unit cell. Most of the solvent molecules and the polar groups are located at the periphery of the unit cell, away from this hydrophobic region. In fact, the crystal packing results in distinct hydrophobic regions (mainly the peptide molecules) and hydrophilic "channels" (mainly solvent), an arrangement that is similar to those observed in the crystal packing of the other amatoxins.[28] This kind of hydrophobic and hydrophilic interaction between the cyclopeptides could resemble the actual amatoxin–enzyme interactions.

When considering possible differences in the conformation of amatoxin **10** in the crystal and in solution, certain facts should be noted: (1) The bicyclic frame and the six intramolecular hydrogen bonds impose a particular favorable molecular con-

(42) Ramakrishnan, C.; Pasad, N. *Int. J. Peptide Protein Res.* **1971**, *3*, 209.

(43) Benedetti, E. In "Chemistry and Biochemistry of Amino Acids, Peptides, and Proteins"; Weinstein, B., Ed.; Marcel Dekker: New York, 1982; Vol. 6, pp 105–184.

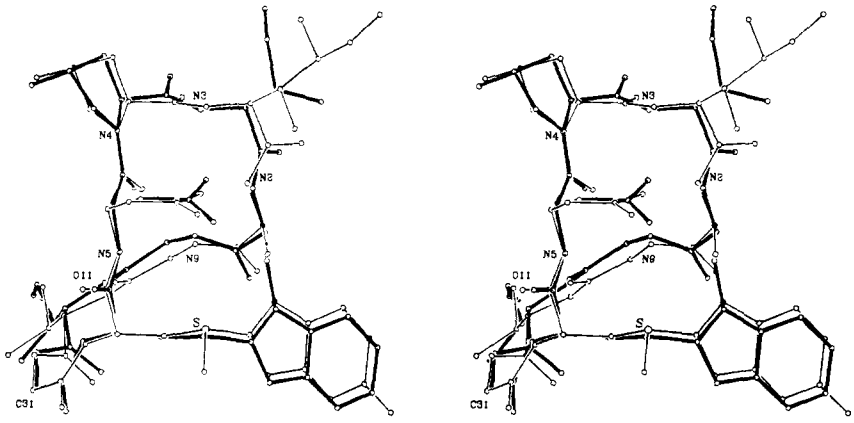

Figure 7. Stereoview of the crystal structure of β-amanitin (**2**) (thin line) superimposed, with the best rms fit, on the crystal structure of **10** (thick line).

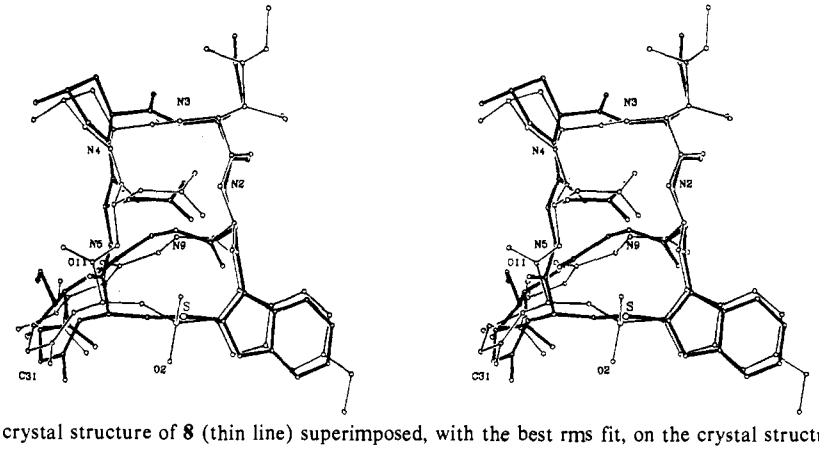

Figure 8. Stereoview of the crystal structure of **8** (thin line) superimposed, with the best rms fit, on the crystal structure of **10** (thick line).

formation, leaving relatively little conformational flexibility. (2) The five solvent molecules present in the crystal per cyclic peptide and their extensive and branched interactions probably resemble, to some extent, the environment in solution. (3) Parallel solid-state–solution studies on related amatoxin derivatives[11,12,14] demonstrated that their structures in the crystal are very similar to their structures in solution. (4) The backbone conformational angles of **10** in the crystal compare relatively well with those of another related thioether amatoxin derivative (**9**) in Me_2SO solution.[14] We therefore believe that the crystal structure of **10**, reported here, closely represents the "true" structure in solution or in biological fluids.

Discussion

The crystal structure of **10** verifies the close structural similarities among amatoxin derivatives. The best fit of the structure of **10** and the structure of β-amanitin[11] by least-squares rotation methods[44,45] gives a rms deviation of 0.62 Å between the 59 related non-hydrogen atoms in the structures. The largest deviation between these two structures takes place in the side chain of residue 3. A similar fit in which atoms C(15), C(16), and C(17) (of the Ile-3 side chain) are not included in the compared molecules gives a rms deviation of only 0.36 Å between the 56 related atoms. Superposition of the two structures after such fit is shown in Figure 7, where the major conformational difference in side chain 3 is demonstrated. Additionally, there is a slight difference in the conformation of the Asp/Asn (in β-amanitin and **10**, respectively) side chain, which is significant enough to add another H bond between N(3)–H and O(10) and strengthen the N(2)–H···O(10) H bond (Table VI) in the molecule of **10**.

The structure of amatoxin **8** (which has been shown to be almost identical with the structure of amatoxin **7**[14,28]) and the structure of **10** were also compared by an analogous fitting procedure. The best fit, including all the 60 common non-hydrogen atoms, gives a rms deviation of 0.69 Å and indicates large differences in the relative positions of C(17) of side chain 3 and O(11) of a main-chain carbonyl group. Ignoring these two atoms in the least-squares fit gives a rms deviation of 0.54 Å between the remaining 58 atoms. Superposition of the two molecules after such rotation is shown in Figure 8. This superposition demonstrates that except for the mismatch of C(17) (which is expected because of the disorder problem) and a slight conformational "twist" of the sulfur bridge, the only significant conformational change between the structures of **10** and **8** is a difference of about 104° in the orientation of the peptide bond consisting of N(5), C(27), and O(11). A similar rotation of this peptide bond plane has been observed between the structures of β-amanitin and amatoxin **8** (and amatoxin **7**),[14] caused probably by hydrogen bonding between N(5)–H and the *S* oxygen on the sulfur in **8** (and **7**). Hence the crystal structure of **10** supports the theory that the "normal" conformation of the peptide bond between residue 8 and residue 1 in amatoxins is similar to that observed in β-amanitin, and it is only in the presence of an *S* oxygen on the sulfur (*S* sulfoxide or sulfone) that this rotation occurs.

On the basis of circular dichroism (CD) and optical rotatory dispersion (ORD) studies of amatoxins in solution,[46] it has been suggested that neither the lack of the two hydroxyl groups (in amanullin (**4**)) nor the lack of the terminal hydroxymethyl (in dehydroxymethyl-α-amanitin) has any influence on the conformation of amatoxins. It also has been shown by NMR and crystallographic analysis[14] that the nature of the sulfur bridge has relatively little effect (aside from rotation of one of the peptide

(44) Kabsch, W. *Acta Crystallogr., Sect. A* **1976**, *A32*, 922.
(45) Kabsch, W. *Acta Crystallogr., Sect. A* **1978**, *A34*, 827.
(46) Faulstich, H.; Bloching, M.; Zobeley, S.; Wieland, Th. *Experimentia* **1973**, *29*, 1230.

bonds, as mentioned above) on the overall molecular conformation. Both of these studies as well as K_i and toxicity measurements[6] indicate that the hydroxyl group on the tryptophan 6′ position, which is present in all natural amatoxins except amanin and amaninamide, does not affect either conformation or biological activity.

Thus, the crystal structure of **10**, which is shown to be very similar to the structure of β-amanitin, supports these interpretations and demonstrates specifically that a derivative with isoleucine in position 3, tryptophan in position 4, and thioether group at the bridge still retains the general overall conformation of active amatoxins.

The reduction in binding affinity (about 30-fold) of **10** to RNA polymerase and lack of toxicity, relative to α-amanatin, are therefore *not* related to conformation. Since the presence of the thioether group and the lack of 6′-hydroxyl at the tryptophan have not affected the binding affinity or toxicity in other derivatives,[6,13] the observed decrease in activity of **10** could be associated with the nature of side chain 3 alone. Furthermore, the decrease in biological activity of the naturally occurring amatoxins amanullin (**4**) and amanullinic acid, and similar synthetic derviatives with altered side chain 3, is very likely due to the nature of side chain 3 and not due to different "inactive" overall conformations.

It seems unlikely that the local conformation of side chain 3 (which has been shown to vary among derviatives) influences the "fit" to the binding site of the enzyme. Only a relatively low rotational barrier (≈2.0 kcal/mol[29]) is expected around the α–β bond and the β–γ1 bond, consistent with the large temperature factors and partial disorder of the relevant atoms in the structures of β-amanitin and **10**.

A more likely possibility, mentioned before,[6,7] is the formation of a direct hydrogen bond between the γ-hydroxy group side chain 3 (present in active amatoxins) and a matching group in the binding site of the enzyme. The lack of this important interaction with the enzyme could account for the reduced affinity of **10** and similar derivatives and could also contribute to the decrease in toxicity.

As already discussed before,[6,13] there is no direct correlation between binding affinities of amatoxins and their toxicities. At least for some amatoxins, as noted above, the observed reduction in toxicity is significantly larger than expected from the reduction in binding affinity, as is the case with compound **10**. Thus, factors other than the binding to the enzyme may influence the toxicity of amatoxins;[13] these factors may include the ability to penetrate the cell or the membrane of the nucleous. In particular, compound **10** lacks three peripheral hydroxy groups, which might affect its ability to cross hydrophilic regions.

We have shown that molecule **10**, like most of the other amatoxin derivatives, is conformationally stable and relatively unstrained. It seems therefore unlikely that any signficant conformational changes occur inside the cell.

Acknowledgment. We thank R. Dumas for technical help in formatting the manuscript, the National Institutes of Health (Grant GM06920) for support, and the National Science Foundation (Grant PCM 77-1398) for initial support of the computational laboratory.

Registry No. 10, 59409-08-4.

Supplementary Material Available: A list of observed and calculated structure factors (Table S1), a list of coordinates and temperature factors for all hydrogen atoms (Table S2), a list of bond lengths involving hydrogen atoms (Table S3), a list of the torsion angles of the peptide (Table S4), and a stereodiagram of the final structure of **10** superimposed on the initial (molecular replacement) model (Figure S1) (28 pages). Ordering information is given on any current masthead page.

Communications to the Editor

Heat of Formation of Diphenylcyclopropenone by Photoacoustic Calorimetry

Joseph J. Grabowski, John D. Simon, and Kevin S. Peters*

Department of Chemistry, Harvard University
Cambridge, Massachusetts 02138
Received April 3, 1984

Since the first reports of the syntheses of cyclopropenone and its derivatives[1] there has been a great deal of interest in the chemistry and physical properties of this class of molecules.[2] One area of interest is the resonance stabilization energy provided by the delocalization of electron density.[3] One criterion used for establishing the magnitude of the resonance stabilization energy is the difference in energy between the experimentally obtained heat of formation of a molecule and a predicted heat of formation derived from an estimate of the strain in the molecule and a hypothetical heat of formation of the molecule ignoring any strain or resonance energy. On the basis of photoacoustic calorimetric measurements, we wish to report for diphenylcyclopropenone (DPCP) a resonance stabilization energy of 11 kcal mol^{-1}. The heat of formation of 86 ± 4 kcal mol^{-1} for DPCP is derived from the enthalpy of reaction for the photodissociation of DPCP to diphenylacetylene and carbon monoxide (eq 1).

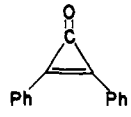

$$\xrightarrow[\text{benzene}]{h\nu} \text{Ph–C}\equiv\text{C–Ph} + \text{CO} \qquad (1)$$

Photoacoustic calorimetry is a method whereby one can determine the reaction enthalpy for ground-state reactants forming photogenerated products that are either stable molecules (as in this case) or have only transient existence.[4] The experiment involves integrating an early portion of an acoustic wave that is generated when heat is released by a molecule following absorption of a photon and consequential reaction. The acoustic wave thus generated is detected by a piezoelectric transducer,[5] amplified,

*Current address: Department of Chemistry, University of Colorado, Boulder, CO 80309.

(1) (a) Breslow, R.; Haynie, R.; Mirra, J. *J. Am. Chem. Soc.* **1959**, *81*, 247. (b) Vol'pin, M. E.; Koreschkov, Yu, D.; Kursanov, D. N. *Izv. Akad. Nauk SSSR, Ser. Khim.* **1959**, 560.
(2) Potts, K. T.; Baum, J. S. *Chem. Rev.* **1974**, *74*, 189–213.
(3) Greenberg, A.; Tomkins, R. P. T.; Dobrovolny, M.; Liebman, J. F. *J. Am. Chem. Soc.* **1983**, *105*, 6855–6858.
(4) (a) Rothberg, L. J.; Simon, J. D.; Bernstein, M.; Peters, K. S. *J. Am. Chem. Soc.* **1983**, *105*, 3464–3468. (b) Simon, J. D.; Peters, K. S. *Ibid.* **1983**, *105*, 5156–5158. In previous studies, we has assumed $1 - 10^{-A} = A$ for small absorbances.
(5) Patel, C. K. N.; Tam, A. C. *Rev. Mod. Phys.* **1981**, *53*, 517–550.
(6) Sandros, K. *Acta Chem. Scand.* **1969**, *23*, 2815–2829.
(7) Turro, N. J.; Lee, C.-G. *Mol. Photochem.* **1972**, *4*, 427–435.
(8) Ermolaev, V.; Terenin, A. *J. Chim. Phys.* **1958**, *55*, 698–704.
(9) Gordon, A. J.; Ford, R. A. "The Chemist's Companion"; Wiley-Interscience: New York, 1977.
(10) Beens, H.; Weller, A. In "Organic Molecular Photophysics"; Birks, J. B., Ed.; Wiley: New York, 1975; Vol. 2.

0002-7863/84/1506-4615$01.50/0